Limitations of the Potential Step Technique to Impedance Measurements Using Discrete Time Fourier Transform

ARTICLE *in* ANALYTICAL CHEMISTRY · OCTOBER 2004

Impact Factor: 5.64 · DOI: 10.1021/ac0493929 · Source: PubMed

2 AUTHORS, INCLUDING:

Andrzej Lasia
Université de Sherbrooke
150 PUBLICATIONS **3,974** CITATIONS

Anal. Chem. **2004,** *76,* 5033−5038

Limitations of the Potential Step Technique to Impedance Measurements Using Discrete Time Fourier Transform

Rafał Jurczakowski† and Andrzej Lasia*

Département de chimie, Université de Sherbrooke, Sherbrooke, Québec, Canada, J1K 2R1

Recently, a new method of measuring impedance of electrochemical systems was proposed in the literature by Yoo and Park (Yoo, J.-S.; Park, S.-M. *Anal. Chem.* 2000, *72,* 2035). It is based on the analysis of system response to a potential step. Differentiation of the applied potential step and the current response in the time domain followed by applying Fourier transform to both signals allows for determination of the system's impedance. It has been proposed that the measurements carried out in a short time period permit the determination of the system's impedance in the whole frequency range. The aim of the present work was to verify the validity of the impedance spectra obtained using this method, as well as to establish the conditions for which the method may be used. This method was tested using simulated data for a simple ideally polarized electrode and a simple one-electron redox system in the solution. The results show that the reliable impedance spectra may be obtained only for frequencies between $1/(N\Delta t)$ and $1/(2\Delta t)$, where Δt denotes the sampling time and N is the number of points acquired during the experiment. However, the artifacts are generated when the experimental data are extrapolated to lower frequencies.

Among the techniques allowing the study of electrochemical systems, impedance spectroscopy keeps a central place. Impedance measurements are usually performed by sequentially sweeping the frequencies and determining the impedance at one frequency at a time. Alternatively, a range of frequencies can be used at the same time by applying such excitation as a white noise or a sum of the selected sinusoidal perturbations of different frequencies.[2,3] In such cases, the perturbation and the system's response must be transformed into frequency domain, using Fourier transform. It is known that the so-called fast Fourier transform (FFT)[2−6] is the most efficient digital algorithm to carry out such transformation. White noise or a computer-generated pseudorandom white noise contains many frequencies, but single-frequency components have relatively low amplitudes and a long data acquisition time is necessary to obtain reliable results.[3]

Another possibility is to use pulse perturbation[3,7] because its Fourier transform contains all the frequencies. However, it is difficult to apply Dirac's δ function perturbation to the system and a short pulse of duration Δt is always applied. However, it was shown that even low-level noise significantly disturbs the impedance spectra measured using this method.[3] Similarly to the pulse perturbation, it is possible to apply a potential step and Fourier transform its first derivative versus time because the derivative of the step is the Dirac's δ function. This method was theoretically analyzed by Gabrielli et al.,[8] who found that this method suffers from bias errors due to the limited integration time and random digital errors due to limitation of the dynamic range of the calculated spectrum. This method is very inaccurate in the high-frequency range, and the systematic errors are inherent to the signal processing. This technique was recently applied in practice by Mochalov and Kolosnitsyn,[9] who constructed a galvanostatic pulse apparatus to measure the electrochemical impedance measurements.

Recently, Yoo and Park[1,10,11] introduced a new method of determination of impedance spectra based on the discrete time Fourier transform (DTFT) of the derivative of the potential step function. The authors used a very short data acquisition time and extrapolated the response to a wide frequency range using DTFT. Since other methods mentioned above are much more time-consuming, this technique would be very advantageous to determine the full impedance spectra, including information about very low frequencies, for systems changing in time, from the measurements carried in a very short time period. However, spectra obtained using this technique were different from the regular impedance spectra, as they did not contain any influence of the mass-transfer impedance. Problems related to this technique were discussed in the letters to the Editor.[12,13]

The aim of the present paper is to verify the validity of this method and to establish the conditions at which it may be used. Theoretical simulations of current−time curves were performed

* To whom all correspondence should be addressed. e-mail: a.lasia@usherbrooke.ca. Tel.: 819-821-7097. Fax: 819-821-8017.

† On leave from University of Warsaw, Department of Chemistry, ul. Pasteura 1, PL-02-093 Warsaw, Poland.

(1) Yoo, J.-S.; Park, S.-M. *Anal. Chem.* **2000**, *72,* 2035.
(2) Creason, S. C.; Hayes, J. W.; Smith, D. E. *J. Electroanal. Chem.* **1973**, *47,* 9.
(3) (a) Popkirov, G. S.; Schindler, R. N. *Bulg. Chem. Commun.* **1994**, *27,* 459. (b) Popkirov, G. S.; Schindler, R. N. *Rev. Sci. Instrum.* **1993**, *64,* 3111.
(4) Cooley, J. W.; Tukey, J. W. *Math. Comput.* **1965**, *19,* 297.
(5) Gold, B.; Rader, C. M. *Digital Processing of Signals*; McGraw-Hill: New York, 1969.
(6) Birgham, E. O. *The Fast Fourier Transform*; Prentice-Hall: Englewood Cliffs, NJ, 1974.
(7) Lasia, A. In *Modern Aspects of Electrochemistry*; Conway, B. E., Bockris, J. O'M., White, R. E., Eds.; Kluwer Academic/Plenum Publishers: New York, 1999; Vol. 32, p 143.
(8) Gabrielli, C.; Keddam, M.; Lizee, J. F. *J. Electroanal. Chem.* **1986**, *205,* 59.
(9) Mochalov, S. E.; Kolosnitsyn, V. S. *Instrum. Exp. Tech.* **2000**, *43,* 53.
(10) Yoo, J.-S.; Song, I.; Lee, J.-H.; Park, S.-M. *Anal. Chem.* **2003**, *75,* 3294.
(11) Park, S.-M.; Yoo, J.-S. *Anal. Chem.* **2003**, *75,* 455A.
(12) Lasia, A. *Anal. Chem.* **2001**, *73* 4059.

10.1021/ac0493929 CCC: $27.50
Published on Web 07/14/2004

for a simple ideally polarized electrode and a redox system in the solution, and the numerically obtained impedances were compared with those theoretically predicted.

CURRENTS AND POTENTIALS IN THE TIME DOMAIN

Data used for computations of the impedance spectra consist of a series of N (from $i = 0$ to $N - 1$) data points of current, measured at the constant interval of Δt, $I(i\Delta t)$, which are the response to the potential step of a small amplitude of 10 mV. Current series were generated using (a) known kinetic equations for chronoamperometry and (b) digital simulations of the electrochemical kinetic−diffusional process, and both methods gave the same results. The currents were calculated for the sampling times of 0.1−10 μs. Numerical calculation of the first derivative of the potential excitation and the system's current response were performed using the following equation:

$$S'(i\Delta t) = \frac{S[(i+1)\Delta t] - S[(i-1)\Delta t]}{2\Delta t} \qquad (1)$$

where S is the measured signal (potential or current). The first derivative of the potential perturbation has the shape of a pulse of a very high magnitude, and it approaches the shape Dirac's δ function with decrease in the time step, Δt. Potential pulse E_p obtained in this way has nonzero values equals to $\Delta E/(2\Delta t)$ only for time between 0 and Δt, and it is equal to zero elsewhere:

$$\frac{dE}{dt}(i\Delta t) = E'(i\Delta t) = E_p = \begin{bmatrix} \Delta E/2\Delta t & 0 \le N \le 1 \\ 0 & \text{otherwise} \end{bmatrix} \qquad (2)$$

FOURIER ANALYSIS

The potential pulse perturbation E_p, and the derivative of current response $I'(i\Delta t)$ are discrete time signals $f(i)$ in the time domain. The derivative signals $E'(i\Delta t)$ and $I'(i\Delta t)$ must be Fourier transformed into the frequency domain, $F(\omega)$. There are a number of algorithms allowing this procedure, among them the FFT is widely used as it allows reduction in the number of calculations. It should be stressed here that analysis in the time $t_{total} = N\Delta t$ gives the information about frequencies between $1/(N\Delta t)$ and the Nyquist frequency $1/(2\Delta t)$[6] and there is no information about the frequencies lower than $1/(N\Delta t)$. In a similar way, the DTFT of the function $f(t)$ consisting of N points can be used to transform the data:[1,6,14]

$$F(\omega) = \sum_{i=0}^{N-1} f(i) e^{-j\omega i\Delta t} \qquad (3)$$

where $f(i)$ is the ith observed signal, Δt denotes the sampling interval, ω is the angular frequency, and j is the imaginary unit. This function is discrete in time and continuous in frequency. The difference between FFT and DTFT is that the latter can be calculated for any frequency, even outside the range for which information exists in the experimental data. Using eq 3, one may find that at the frequencies lower than $1/2\Delta t$ a constant response is obtained from the potential pulse in the frequency space

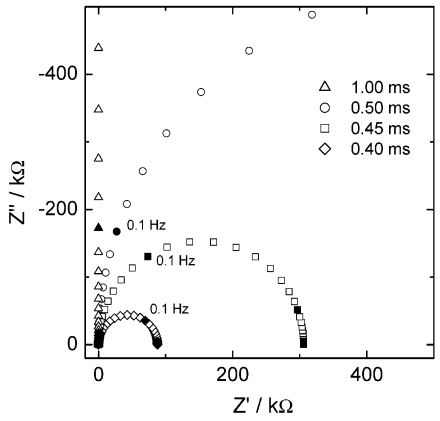

Figure 1. Complex plane plots for the R_s-C_{dl} connection in series ($R_s = 4$ Ω, $C_{dl} = 10$ μF) for various total data acquisition times t_{total}: (◇) 0.4, (□) 0.45, (○) 0.5, and (△) 1 ms and the sampling time $\Delta t = 1$ μs. Solid symbols represent the decades of frequencies.

indicating that, theoretically, the obtained response contains information about all these frequencies.[7]

IDEALLY POLARIZABLE ELECTRODE

An ideally polarizable electrode may be represented by the connection of the solution resistance, R_s, in series with the double layer capacitance, C_{dl}. Impedance of this system is $\hat{Z} = R_s + 1/j\omega C_{dl}$, and the Nyquist plot of the impedance constitutes a straight line perpendicular to the Z' axis.[7] In this case, the current, I, relaxation in the time domain due to the application of the potential step, ΔE, can be described as

$$I = U(t)(\Delta E/R_s)e^{-t/R_sC_{dl}} \qquad (4)$$

where $U(t)$ is the unit step function. According to eq 4, the current decreases exponentially to zero but does not reach any steady-state value, and therefore, its first derivative actually never drops to zero. The first derivative of current response is

$$\frac{dI}{dt} = \frac{\Delta E}{R_s}e^{-t/R_sC_{dl}}\left(\delta(t) - \frac{U(t)}{R_sC_{dl}}\right) \qquad (5)$$

where $\delta(t)$ is the Dirac delta function. This response contains two parts: one Dirac's δ function and another an exponential decay. The electrode impedance may be obtained as $\hat{Z}(\omega) = F[E(t)]/F[I(t)]$, where operator F denotes Fourier transform. Numerical calculations of the impedance using DTFT produce the complex plane plots displayed in Figure 1. A general shape of the obtained complex plane plots is a semicircle; however, at higher frequencies they look like a straight line at 90°. The radius of the semicircle depends on the total data acquisition time and it changes from 87 kΩ for $t_{total} = 0.4$ ms, 303 kΩ for 0.45 ms, and over 1 MΩ for 0.5 ms. Only extrapolation of the obtained plots to the frequencies much lower than $f = 1/t_{total} = 1/N\Delta t$ causes formation of semicircles. This behavior is due to the truncation of the derivative in eq 5 and extrapolation of the DTFT to lower frequencies. The Bode plots obtained from the simulations of the ideally polarizable electrode are presented in Figure 2. Here, extrapolation to the frequencies lower than $1/t_{total}$ may initially show the correct results, but at certain lower frequencies, deviation from the theoretical continuous line occurs and the formation of a semicircle on the complex plane plots is observed. Therefore, it is risky

(13) Yoo, J.-S.; Park, S.-M. *Anal. Chem.* **2001**, *73* 4060.
(14) Gabel, R. A.; Roberts, R. A. *Signals and Linear Systems*; Wiley: New York, 1987.

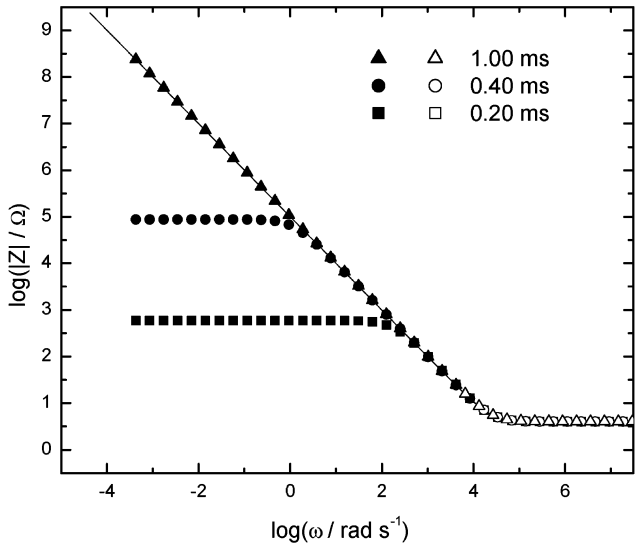

Figure 2. Bode magnitude plots for the R_s-C_{dl} connection in series ($R_s = 4\ \Omega$, $C_{dl} = 10\ \mu$F) for different total data acquisition time, t_{total} = (▲, △) 1.0, (●, ○) 0.4, and (■, □), 0.2 ms. Open symbols indicate the frequency range from $1/t_{total}$ to $1/(2\ \Delta t)$; full symbols the extrapolation of the experimental data to lower frequencies; a continuous line indicated theoretical dependence for the R_s-C_{dl} circuit.

to extrapolate the data outside the experimentally measured frequencies, which may lead to the appearance of artifacts (semicircles).

IMPEDANCE OF THE ELECTROCHEMICAL REDOX REACTION

Model. As the next step, impedance of a simple one-electron reaction

$$\mathrm{Ox} + e \underset{k_b}{\overset{k_f}{\rightleftharpoons}} \mathrm{Red} \tag{6}$$

was explicitly modeled for different heterogeneous rates constants k_f, k_b. For this process, the expression for the faradaic current density may be written as

$$I_f = nFc_{ox}(0, t) \tag{7}$$

The diffusional transport of species ox and red was assumed to obey Ficks's law for linear diffusion:

$$\frac{\partial c_{ox}}{\partial t} = D_{ox}\frac{\partial^2 c_{ox}}{\partial x^2} \tag{8}$$

$$\frac{\partial c_{red}}{\partial t} = D_{red}\frac{\partial^2 c_{red}}{\partial x^2} \tag{9}$$

Potential Step. The chronamperometric current density in the time domain was calculated using digital simulations by means of the finite difference method and on the basis of the well-known general solution for electrode processes[15,16] according to which the current relaxation due to a potential step is described as

$$I_f = nF(c^0_{ox}k_f - c^0_{red}k_b)\exp(\kappa^2 t)\ \mathrm{erfc}(\kappa t^{1/2}) \tag{10}$$

where

$$\kappa = (k_f/D_{ox}{}^{1/2}) + (k_b/D_{red}{}^{1/2}) \tag{11}$$

c^0_{ox} and c^0_{red} are the bulk concentrations of ox and red forms, k_f and k_b are the heterogeneous rate constants and D_{ox} and D_{red} are the diffusion coefficients.

Current−time curves were calculated for the potential step of 10 mV from E_1 to E_2, and the concentrations of the reactive species c^0_{ox} and c^0_{red} at the potential E_1, in eq 10, were estimated by assuming the equilibrium state that is from the Nernst equation for the initial bulk concentration of ox $c^0_{ox} = 50$ mM. Using concentration profiles from the digital simulations of the diffusion−kinetic problem gave the same results. Next, the capacitive current, eq 4, was added to the faradaic current. An example of the obtained chronoamperometric curve is presented in Figure 3. The parameters used for simulation of this curve are shown in the caption. The observed current decreases rapidly with time and, after ∼100 μs, it reaches what looks like a steady state.

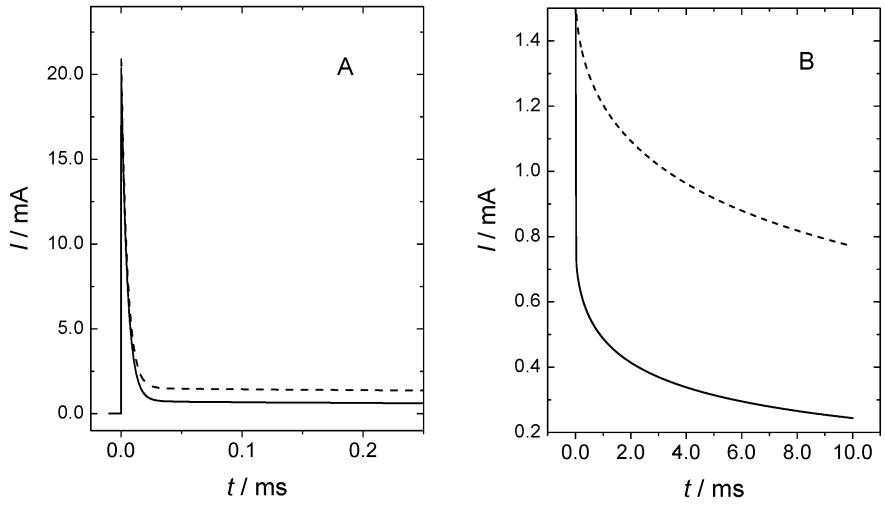

Figure 3. Chronoamperometric current due to a potential step for a quasi-reversible system at two potentials $E_1 - E_0$: (- - -) 50 mV, (—) 90 mV, $k_s = 5 \times 10^{-3}$ cm·s^{-1}, initial $c^0_{ox} = 50$ mM, $D_{ox} = D_{red} = 5 \times 10^{-6}$ cm^2 s^{-1}, $C_{dl} = 10\ \mu$F, $R_s = 0.5\ \Omega$, $t_{total} = 10$ ms, and $\Delta t = 1 \times 10^{-7}$ s. (A) for $t = 0-0.25$ ms and (B) for $t = 0-10$ ms, i.e., continuation of (A).

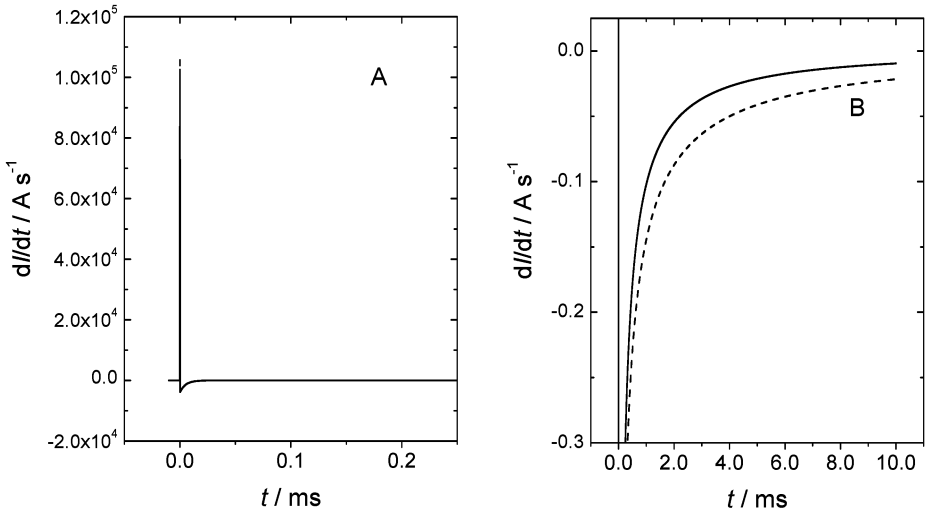

Figure 4. First derivative of the chronoamperometric currents from Figure 3.

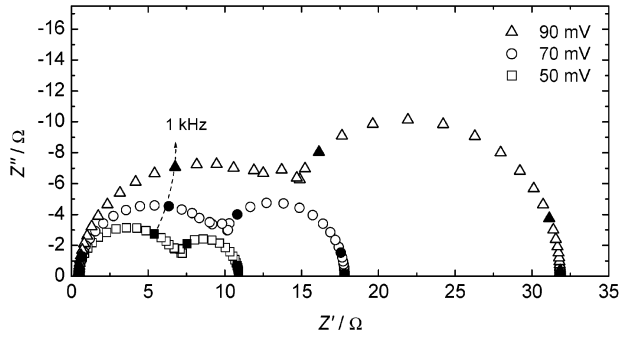

Figure 5. Complex plane plots of impedance calculated using DTFT of the first derivative of the chronoamperometric currents from Figure 4; frequency range 1 MHz to 1 μHz, $E_1 - E_0$: (□) 50, (○) 70, and (Δ) 90 mV; solid symbols represent the decades of frequencies. Total data acquisition time $t_{total} = 5$ ms. Other parameters are listed in the caption to Figure 3.

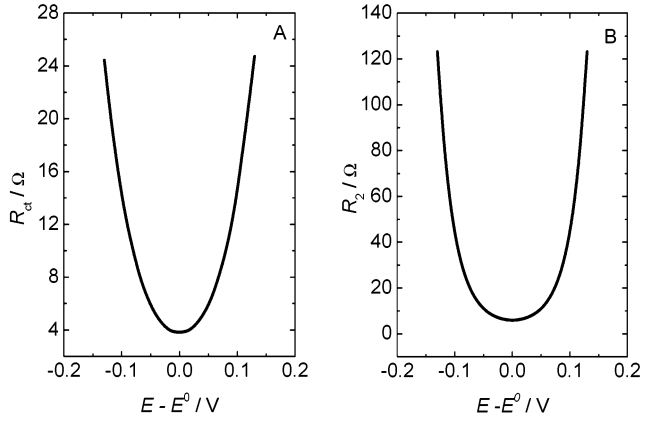

Figure 6. Dependence of the diameter of the high frequency, R_{ct}, and the low frequency, R_2, semicircles observed on the complex plane plots, calculated from the first derivative of the chronoamperometric currents, total data acquisition time $t_{total} = 5$ ms; other parameters as in the caption to Figure 3.

However, after changing the current scale, it is evident that the current decreases continuously following eq 10. Similar behavior can be observed for the first derivative of the current, Figure 4. This derivative transient is analogous to that in Figure 6 of ref 1. The observed behavior shows that the assumption that for $N_0 < N < \infty$ (where N_0 is the experimental number of points taken to analysis) current equals zero is an approximation only and extrapolation of the impedances to lower frequencies using DTFT might not be justified.

Impedance. Taking into account data truncated at $t_{total} = 5$ ms, the electrochemical impedance was calculated in the frequency range from 1 MHz to 1 μHz using DTFT of the first derivative of chronoamperometric current. Figure 5 presents complex plane plots obtained in this way at different potentials ($E - E^0$). Two semicircles are present on the complex plane plots for a simple one-electron redox process. The diameter of both semicircles depends on dc potential, Figure 6, with the minimum at the standard potential. However, only the diameter of the second, low-frequency, semicircle, R_2, increases with the total data acquisition time, t_{total}. It is interesting to note that a linear relationship exists between its radius and the square root of the total acquisition time, Figure 7. This analysis shows that the appearance of the low-frequency semicircle is simply an artifact related to the truncation of data in time domain.

When the total time, t_{total}, is increased to more than 50 ms, the low-frequency semicircle becomes deformed and a straight line at 45° due to the Warburg impedance appears. Figure 8 shows the impedance spectra for different total data acquisition times; the Warburg impedance is clearly visible. This straight-line segment at 45° becomes longer as the total time increases and approaches the theoretical Warburg impedance (straight line at 45°). Figure 9 shows the Bode phase-angle plot of the calculated and theoretical impedances for this system; circles represent the result of calculation of the impedances using DTFT, open circles correspond to the frequency range form $1/(N\Delta t)$ to $1/(2\Delta t)$, and the full circles are for frequencies below $1/(N\Delta t)$. It is clearly visible that all the values represented by full points and determined at extrapolated frequencies are erroneous. Thus, the formation of the second semicircle is an artifact due to extrapolation of the impedances below the lowest experimental angular frequency, in this case $2\pi/(N\Delta t) = 2\pi/(0.4\text{ s}) = 15.70$ rad·s^{-1}. Similar Bode phase-angle spectra were obtained for other t_{total} values. In these cases, the erroneous results were observed below frequencies 31.4 and 7.85 rad·s^{-1} for the total times of 200 and 800 ms, respectively, corresponding to $2\pi/t_{total}$.

The origin of this behavior is rather easy to understand; the assumption that the first derivative is equal to zero at time t_{total} means that at this time t_{total} the system attains a steady state and

(15) Delahay, P. *J. Am. Chem. Soc.* **1953**, *75*, 1430.
(16) Oldham, K. B. *J. Electroanal. Chem.* **1982**, *136*, 175.

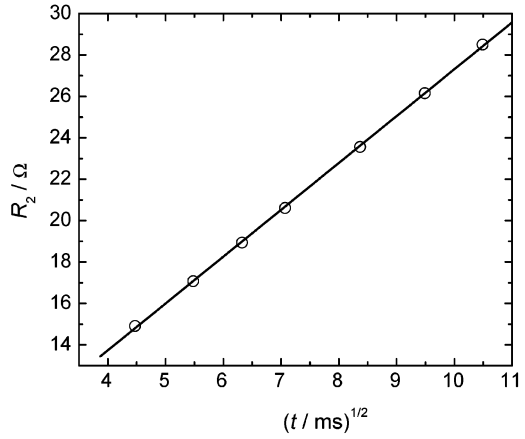

Figure 7. Dependence of the diameter of the second semicircle on the square root of the total data acquisition time, t_{total}; $E_1 - E_0 =$ 50 mV, $k_s = 5 \times 10^{-3}$ cm·s^{-1}, initial $c^0_{ox} = 50$ mM, $D_{ox} = D_{red} = 5 \times 10^{-6}$ cm^2·s^{-1}, and $\Delta t = 1 \times 10^{-6}$ s.

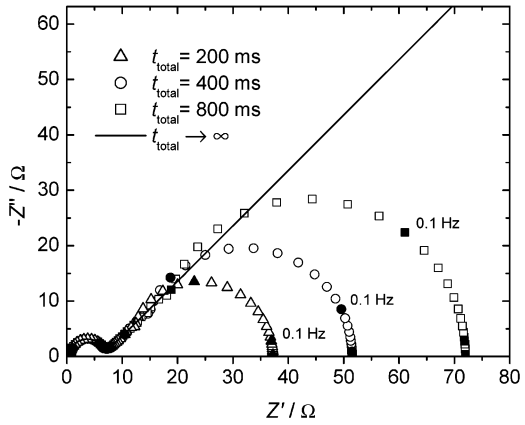

Figure 8. Nyquist impedance plots calculated for different total experiment times, t_{total}: (△) 200, (○) 400, and (□) 800 ms; rate constant $k_s = 5 \times 10^{-3}$ cm·s^{-1}, $D_{ox} = D_{red} = 5 \times 10^{-6}$ cm^2·s^{-1}, t_{total} = 10 ms, $\Delta t = 1 \times 10^{-6}$ s, and $E_1 - E_0 = 40$ mV. Solid symbols represent the decades of frequencies, and continuous line (—) represents the theoretical impedance for this system.

a steady-state current is observed in the time domain. This corresponds to finite-length diffusion, as for the rotating disk electrode. Indeed, the complex plane plots presented in Figure 8 have typical shape for this type of process, displaying kinetic (high-frequency semicircle) and finite length transmissive diffusion at low frequencies.[7] However, at times longer than t_{total} the concentration gradient and its derivative are still changing, and although these changes are becoming slower at longer times, they never become equal to zero as long as the linear diffusion is considered.

Time at which the Warburg impedance starts to appear on the complex plane plots depends on the value of the rate constant of the electrochemical process and concentration of the electroactive species. In the case of the reversible reaction, Warburg impedance is clearly visible at total times shorter then 400 μs. On the other hand, for very slow processes, when $k_s \rightarrow 0$ or $t \rightarrow 0$

$$\exp[\kappa^2 t]\ \mathrm{erfc}[\kappa\sqrt{\tau}] \rightarrow 1 \qquad (12)$$

the faradaic current I_f is close to its initial value

$$I_f \approx nF(k_f c_{ox} - k_b c_{red}) \qquad (13)$$

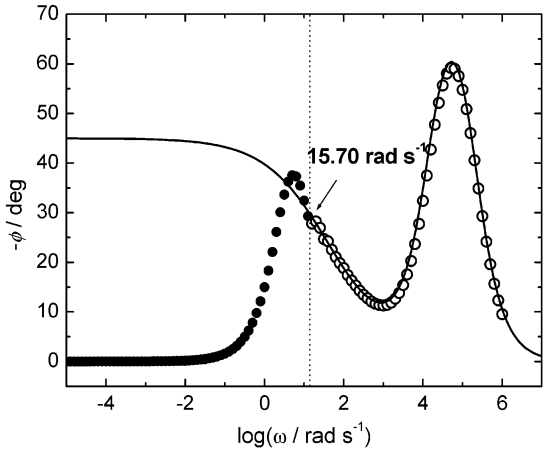

Figure 9. Bode phase-angle plots for $t_{total} = 400$ ms, corresponding to $\omega_{max} = 15.7$ rad·s^{-1}. Circles represent the results obtained using DTFT of the first derivative of the current; (○) in the frequency range from $1/(N\Delta t)$ to $1/(2\Delta t)$, (●) at frequencies lower than $1/(N\Delta t)$; continuous line (—) theoretical impedance for this system.

and for $\omega \rightarrow 0$ and $\Delta E \rightarrow 0$, one can obtain

$$Z_{f,\omega=0} = \frac{\Delta E}{nF(k_f c_{ox} - k_b c_{red})} \approx R_{ct} \qquad (14)$$

Then, using DTFT, one can approximate the charge-transfer resistance. Figure 10 shows the complex plane impedance plots obtained at different total times. At short total times, from 0.1 to ~1 ms, one semicircle of a similar diameter is observed. This diameter is close to the theoretical value of the charge-transfer resistance. From the Bode phase-angle plot in Figure 10B, it is evident that the approximation of the impedance in the frequency range from 6.28×10^4 to ~320 rad·s^{-1} that is outside the experimental frequency range is still good, contrary to the reversible or quasi-reversible case presented in Figure 9. This fact arises from the extrapolation of the beginning of the semicircle, observed already at the frequencies lower than 6.28×10^4 rad s^{-1}, to lower frequencies. However, below the frequency of $\omega =$ 320 rad·s^{-1}, deviation from the theoretical impedance is evident, as only continuation of the semicircle may be obtained from the experimental data because they do not contain any information about the diffusion.

CONCLUSION

It has been shown that the potential step method followed by differentiation of the current and FFT or DTFT may be used to obtain impedance spectra. In view of the results presented above, it is clear that the strictly reliable impedance results may be obtained only in the frequency range from $1/(N\Delta t)$ to $1/(2\Delta t)$, Figure 9. In some cases, it is possible to continue the extrapolation to lower frequencies, Figure 10; however, no new information is obtained.

This method has been proposed to obtain the impedance spectra of the systems, which evolve with time.[1–11,13] Although the use of DTFT allows for simulation of the data in the whole frequency range, it is not possible to get more information than that already present in the experimental current−time data. Extrapolation of impedances below the smallest frequency present in the system, that is, $1/(N\Delta t) = 1/t_{total}$ introduces artifacts, that is for a simple ideally polarized electrode a semicircle is obtained instead of the straight line at 90°, Figure 1, and for a simple

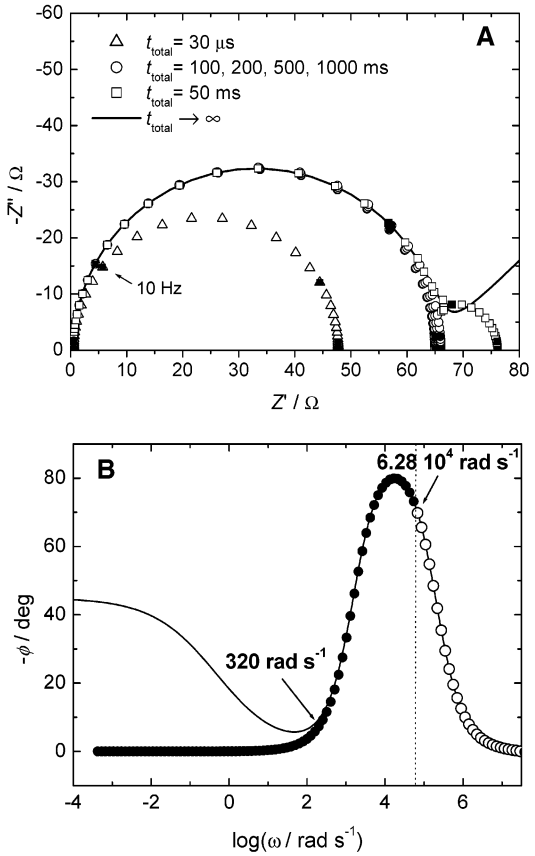

Figure 10. Impedance of the irreversible faradaic reaction; (A) complex plane impedance plots calculated for different total times t_{total}: (△) = 30, (○) 100, 200, 500, and 1000 μs and (□) 50 ms. Solid symbols represent the decades of frequencies; (B) Bode phase-angle plots for the total time $t_{total} = 100\ \mu$s, (○) points in the frequency range form $1/(N\Delta t)$ to $1/(2\Delta t)$, (●) calculated at frequencies lower than $1/(N\Delta t)$; continuous line represents theoretical impedance for this system. Sampling time step $\Delta t = 1 \times 10^{-7}$ s, solution resistance $R_s = 0.5\ \Omega$, $C_{dl} = 10\ \mu$F, $k_s = 5 \times 10^{-4}$ cm·s^{-1}, $D_{ox} = D_{red} = 5 \times 10^{-6}$ cm^2·s^{-1}, and $E - E^0 = 50$ mV.

diffusion−kinetic system two semicircles or one semicircle followed by a semicircle or a skewed semicircle is obtained instead of the typical Randles behavior (semicircle followed by a straight line at 45°), Figure 5 and Figure 8. It should be stressed here that for all impedance plots presented in this paper the imaginary part of impedance Z'' obtained from the real part Z' using Kramers−Kronig transformation is in perfect agreement with the results of straightforward simulation. This result is quite obvious since impedance data have been calculated and extrapolated using DTFT; therefore, such data are always KK transformable.

Yoo and Park applied this method to study the kinetics of the $Fe(CN)_6^{3-/4-}$ system[1] or conducting polymers during continuous cyclic voltammetric experiments.[13] In the case of the $Fe(CN)_6^{3-/4-}$ system, the authors obtained one semicircle on the complex plane plots, but the measurements were conducted during a very short time of 2 ms and the results were extrapolated to 1 mHz. Of course, the authors have not seen any influence of the diffusion (Warburg impedance). It has been shown above that such a procedure introduces artifacts; see Figures 5−8. The kinetics of the $Fe(CN)_6^{3-/4-}$ system in the conditions studied is very fast (high concentration of electroactive species, large electrode surface area). The heterogeneous rate constant of this system in neutral solutions at a platinum electrode was found to be of order of 0.1 cm·s^{-1}; see ref 17 and the references therein. The charge-transfer resistance calculated from this rate constant is very small (0.85 Ω·cm^2 at $E = E°$), which suggests that the semicircle observed by the authors using the DTFT method could be related to the mass transfer; that is, it corresponded to the second semicircle in Figure 5. It should be noticed that for the same experimental conditions but using the classical FRA method the authors observed practically only Warburg impedance (see Figure 8 in ref 1).

The method proposed above may be used to determine impedances in the short experimental times, but the information obtained is limited. Use of longer total experiment times with fast data acquisition is not possible as the chronoamperometric curve decreases rapidly with time and current becomes buried in the experimental noise.

DTFT may be used on a finite interval (0, t_{total}), and the results might be extrapolated to lower frequencies only if the signal is equal to zero at $t > t_{total}$. However, in electrochemical systems, current response on potential excitation is usually infinitely long. When DTFT is employed for computation of impedance in such systems, the spectra give reliable information only about frequencies from $1/(N\Delta t)$ to $1/(2\Delta t)$. The lack of Warburg impedance is simply the effect of unjustified truncation in the time domain of the electrochemical signal.

Because in chronoamperometric measurements the current decreases rapidly with time, this causes a general problem and, in principle, current sensitivity (current scale in the potentiostat) should be changed during the measurement to attain sufficient sensitivity for the current determination. The proposed method is also subject to the experimental errors due to the numerical differentiation, which always increases the noise level. It should be stressed again that although theoretically this method is equivalent to the application of the sum of several frequencies followed by the FFT of the excitation and response signals[2,3,7,18,19] in practice it is inferior because of the systematic errors and errors due to the parasitic noise.[8]

ACKNOWLEDGMENT

Financial support from NSERC is gratefully acknowledged.

Received for review April 22, 2004. Accepted June 3, 2004.

AC0493929

(17) *Encyclopedia of electrochemistry of the elements*; Bard, A. J., Ed.; M. Dekker: New York, 1982; Vol. IX.

(18) Schiewe, J., Házi, J.; Vicente-Beckett, V. A.; Bond, A. M. *J. Electroanal. Chem* **1998**, 129.

(19) (a) Walters, M. J.; Garland, J. E.; Pettit, C. M.; Zimmerman, D. S.; Marr, D. R.; Roy D. *J. Electroanal. Chem*. **2001**, *499*, 49. (b) Garland, J. E.; Assiongbon, K. A.; Pettit, C. M. Emery, S. B.; Roy, D. *Electrochim. Acta* **2002**, *47*, 4113.